

# AST325 Lab 5: Mapping the Milky Way

Shimona Das

Student Number: 1008964943

Group N

March 2025

## Abstract

This paper presents an analysis of the Galactic rotation curve using 21 cm neutral hydrogen (HI) observations obtained from the Carp 12.8m observatory located in Ottawa. By converting the observed frequency  $f$  to radial velocity via the Doppler formula and applying the tangent-point method where the Galactocentric radius is determined by  $R = R_0 \sin(l)$  and the rotation speed by  $V(R) = v_{\text{los}} + V_0 \sin(l)$ , a rotation curve spanning Galactic longitudes from  $3^\circ$  to  $84^\circ$  was subsequently derived. A cubic polynomial fit was used to smooth the derived rotation speeds and capture the rapid increase in velocity at small radii and the subsequent flattening near the solar circle. The results then indicated that the rotation speed rises to approximately  $200\text{--}240 \text{ km s}^{-1}$  at a Galactocentric radius of approximately 8 kpc, again consistent with previous studies and suggestive of an extended mass distribution dominated by a dark matter halo rather than solely by the luminous central bulge. This work demonstrates the effectiveness of the tangent point method in mapping Galactic kinematics and provides valuable insights into the gravitational potential and mass distribution of the Milky Way.

## 1 Introduction

The structure and dynamics of the Milky Way are areas of intense study in astronomy. One of the most powerful tools available for probing the Galactic structure is the observation of the 21 cm line of neutral hydrogen (HI). This hyperfine transition which occurs at a rest frequency of 1420.4 MHz, arises from the energy difference between the parallel and antiparallel alignments of the proton and electron spins in hydrogen atoms. Due to the extremely long lifetime of the excited state, the intrinsic line width is very narrow and also makes the 21 cm line an excellent probe of Doppler shifts caused by the motion of gas in the Galaxy. The Doppler shift, under the non relativistic approximation, can be expressed as

$$v \approx c \frac{f_0 - f}{f_0},$$

where  $c$  is the speed of light,  $f_0$  is the rest frequency, and  $f$  is the observed frequency. This relation allows the conversion of observed frequency shifts to radial velocities and provide insights into the kinematics of the interstellar medium.

An important step in deriving the Galactic rotation curve is the *tangent-point method*. In the first Galactic quadrant ( $0^\circ < l < 90^\circ$ ), the tangent point is the location along the line of sight where the distance to the Galactic centre is minimized. At this point, the Galactocentric radius  $R$  is given by the following formula:

$$R = R_0 \sin(l),$$

here  $R_0$  is the distance from the Sun to the Galactic centre and  $l$  is the Galactic longitude. The corresponding rotation speed can be derived from the observed line of sight velocity  $v_{\text{los}}$  using:

$$V(R) = v_{\text{los}} + V_0 \sin(l),$$

with  $V_0$  representing the local circular speed. These formulas form the basis to construct the rotation curve of the Milky Way and then compare it with expectations from a centrally concentrated mass distribution.

In a system where the mass is primarily concentrated in the central bulge, it would be expected that there is a *Keplerian* decline in orbital speeds, following  $V(R) \propto R^{-1/2}$  at radii beyond the bulge.

However, observations of the Milky Way consistently reveal a nearly flat or gently rising rotation curve out to the solar circle and beyond. This discrepancy strongly indicates the presence of a massive, extended dark matter halo that dominates the gravitational potential at large radii.

This lab report details observations of the 21 cm line, the extraction of radial velocities, and the application of the tangent point method to derive the Galactic rotation curve. The subsequent sections describe the experimental setup, data collection, and processing techniques, ending in a discussion of our findings and their implications for the mass distribution of the Milky Way.

## 2 Data and Observation

Date	Personnel	Notes
24/02/2025	S. Das, M. Pye	Recorded set of data set on Carp 12.8m

Table 1: A summary of observations

Specification	Carp Observatory 12.8m (CCERA)
Location	Carp, Ontario, Canada
Dish Diameter	12.8 meters
Operating Frequency	1420 MHz (21cm Hydrogen Line)
Receiver Type	AirSpy SDR-based backend
Spectral Resolution	$\sim 5$ kHz per channel
Beamwidth	$\sim 0.6$ degrees at 1420 MHz
System Temperature	$\sim 50$ K
Elevation Range	$10^\circ$ to $88^\circ$
Azimuth Range	Full $360^\circ$ rotation
Pointing Accuracy	$\sim 0.1^\circ$
Data Acquisition	Remote-controlled via AB82 station
Observation Mode	Pre-programmed survey or manual pointing
Integration Time	Adjustable (15s minimum recommended)
Dimensions	Fixed-position parabolic dish antenna

Table 2: Properties of the Carp Observatory 12.8m (CCERA)

### Expected Telescope Pointings

Time (UTC)	Gal l (deg)	Gal b (deg)	RA (deg)	Dec (deg)	Alt (deg)	Az (deg)
2025-02-24 14:30:00	3	0	268.15	-26.36	16.47	202.59
2025-02-24 14:31:30	6	0	269.82	-23.77	19.30	202.26
2025-02-24 14:33:00	9	0	271.42	-21.16	22.13	201.93
2025-02-24 14:34:30	12	0	272.97	-18.54	24.95	201.61
2025-02-24 14:36:00	15	0	274.47	-15.90	27.78	201.28
2025-02-24 14:37:30	18	0	275.93	-13.26	30.62	200.94
2025-02-24 14:39:00	21	0	277.36	-10.60	33.45	200.60
2025-02-24 14:40:30	24	0	278.76	-7.94	36.28	200.24
2025-02-24 14:42:00	27	0	280.15	-5.28	39.12	199.86
2025-02-24 14:43:30	30	0	281.52	-2.61	41.95	199.45
2025-02-24 14:45:00	33	0	282.89	0.06	44.78	199.02

Continued on next page

Time (UTC)	Gal l (deg)	Gal b (deg)	RA (deg)	Dec (deg)	Alt (deg)	Az (deg)
2025-02-24 14:46:30	36	0	284.26	2.73	47.61	198.53
2025-02-24 14:48:00	39	0	285.63	5.40	50.43	197.98
2025-02-24 14:49:30	42	0	287.02	8.06	53.26	197.36
2025-02-24 14:51:00	45	0	288.43	10.72	56.07	196.64
2025-02-24 14:52:30	48	0	289.86	13.38	58.89	195.80
2025-02-24 14:54:00	51	0	291.32	16.02	61.69	194.79
2025-02-24 14:55:30	54	0	292.82	18.66	64.48	193.55
2025-02-24 14:57:00	57	0	294.37	21.28	67.25	192.00
2025-02-24 14:58:30	60	0	295.98	23.89	70.01	190.01
2025-02-24 15:00:00	63	0	297.65	26.48	72.73	187.37
2025-02-24 15:01:30	66	0	299.40	29.05	75.39	183.72
2025-02-24 15:03:00	69	0	301.23	31.60	77.96	178.44
2025-02-24 15:04:30	72	0	303.17	34.12	80.37	170.37
2025-02-24 15:06:00	75	0	305.23	36.61	82.46	157.34
2025-02-24 15:07:30	78	0	307.42	39.05	83.89	136.46
2025-02-24 15:09:00	81	0	309.77	41.46	84.15	109.07
2025-02-24 15:10:30	84	0	312.30	43.81	83.11	85.01

Table 3: Expected Telescope Pointings for the 12.8m Carp Observatory on February 24, 2025

### 3 Data Reduction

The raw data for this experiment consisted of binary files containing 21 cm spectral measurements from multiple telescope pointings. In order to prepare these data for analysis, a data reduction process was implemented to correct for instrumental effects and extract the relevant astronomical signals.

The raw binary files were read using Python’s `struct` and `numpy` libraries. Each file contained header information such as the number of frequency channels ( $n_f$ ), the number of time samples ( $n_t$ ), and the telescope’s altitude and azimuth as well as arrays corresponding to the frequency list ( $l_f$ ), time samples ( $l_t$ ), the averaged spectrum ( $s_p$ ), and a baseline ( $b_l$ ). The initial processing step involved subtracting the polynomial fit baseline from the averaged spectrum to obtain a cleaned, baseline-subtracted signal:

$$\text{spectrum}_{\text{corrected}} = s_p - b_l.$$

Initially a polynomial fit and a 1416 Hz baseline was supposed to be applied. However, due to low RFI and the sources being clear and bright, the 1416 Hz did not need to be applied. Next, the frequency axis was converted into a radial velocity axis using the Doppler shift equation, where  $c$  is the speed of light and  $f_0$  is the rest frequency of the HI line (1420.4 MHz). In order to minimise the impact of noise and radio frequency interference (RFI), the data were limited to a velocity range of  $[-300, 300]$  km s $^{-1}$ .

A peak-finding algorithm was then applied to the baseline subtracted spectrum to identify significant features. Thresholds on peak height at 1.0 and prominence at 0.5 also were chosen to ensure that only those peaks likely to correspond to genuine HI emission were selected. For each telescope pointing, which corresponds to a distinct Galactic longitude, the tangent point method was used by selecting the maximum velocity peak. At the tangent point in the first Galactic quadrant, the Galactocentric radius is given by

$$R = R_0 \sin(l),$$

and the rotation speed is calculated as

$$V(R) = v_{\text{los}} + V_0 \sin(l),$$

where  $R_0$  is the Sun’s distance from the Galactic centre,  $V_0$  is the local circular speed, and  $l$  is the Galactic longitude.

To get a decent and smooth representation of the rotation curve, a cubic polynomial was fitted to the derived rotation speeds as a function of Galactocentric radius. A cubic fit was chosen because it provides sufficient flexibility to capture the rapid rise in rotational velocity at small radii along with the subsequent flattening near the solar circle, without over fitting the limited number of data points. The quality of the fit was further assessed by examining the residuals, which helped in quantifying the uncertainties and also identifying systematic deviations.

## 4 Data Analysis

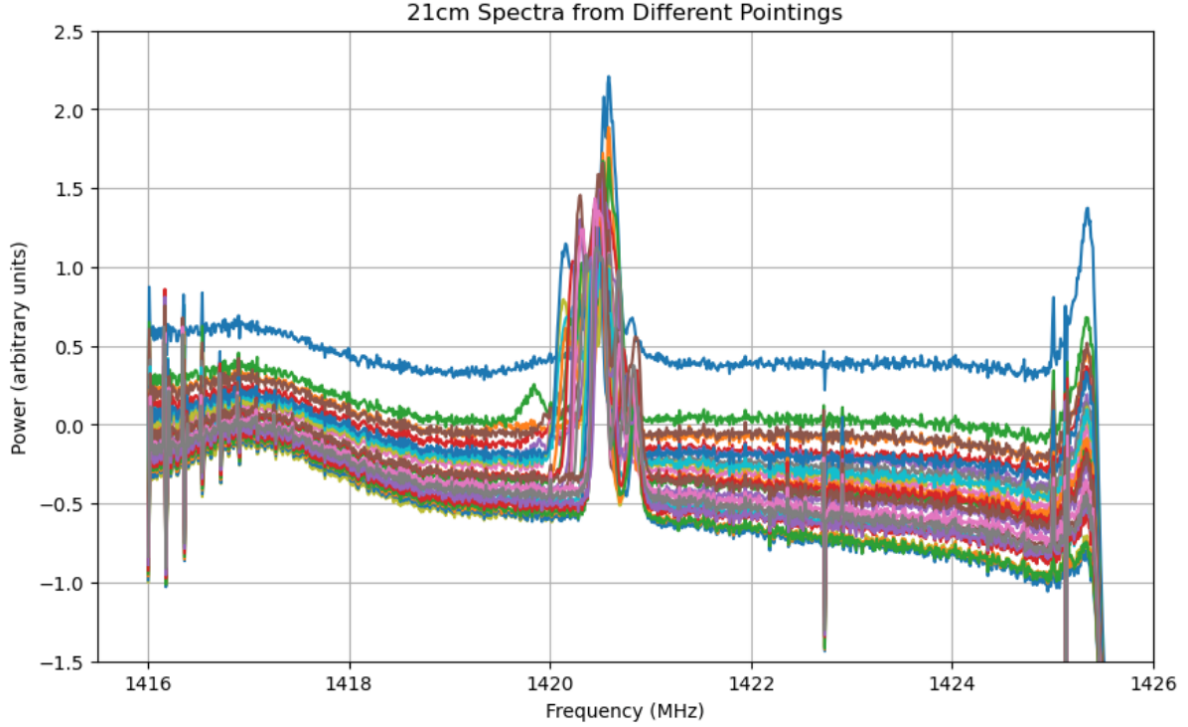


Figure 1: Plot of 21 cm spectra measured at multiple telescope pointings. Each colored trace corresponds to a different pointing direction with the horizontal axis showing frequency (in MHz) near the 1420.4 MHz HI line and the vertical axis which indicates measured power in arbitrary units.

Figure 1 presents the measured 21 cm spectra for multiple telescope pointings from 3 to 84 degrees, with frequency (in MHz) along the horizontal axis and power (in arbitrary units) on the vertical axis. Every colour coded trace corresponds to a different pointing and highlights variations in baseline shape and signal amplitude across the dataset. The strongest feature appears near 1420.4 MHz which is also consistent with the Galactic HI line, while smaller peaks and dips reflect local RFI or residual baseline structure. The plot is scaled to show the full range of the power. Although no explicit error bars are shown here, future improvements might include them to quantify the measurement uncertainties at each frequency channel.

Figure 2 presents a set of 21 cm spectra recorded at different telescope pointings but now displayed as a function of radial velocity. Plotting in velocity units makes it pretty straightforward to identify the primary Galactic neutral hydrogen line near 0 km/s, along with any other approaching or receding components at more negative or positive velocities. Each coloured trace represents a unique pointing with the most prominent peak corresponding to local Galactic HI.

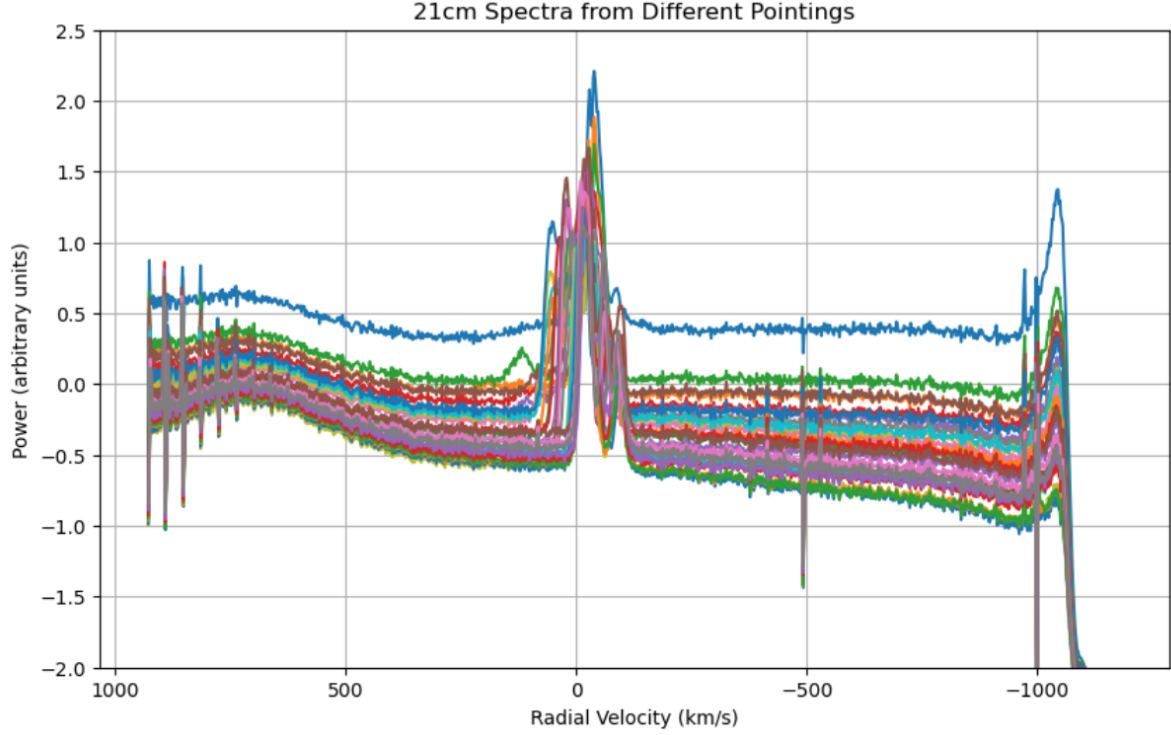


Figure 2: This figure displays 21 cm spectra from different telescope pointings, now plotted against radial velocity ( $\text{km s}^{-1}$ ). Each colour-coded trace corresponds to a unique pointing direction and reveals how the HI line profile and baseline features vary across observations. The prominent peak near zero velocity corresponds to Galactic neutral hydrogen while smaller peaks and dips indicate residual baseline structure or local interference.

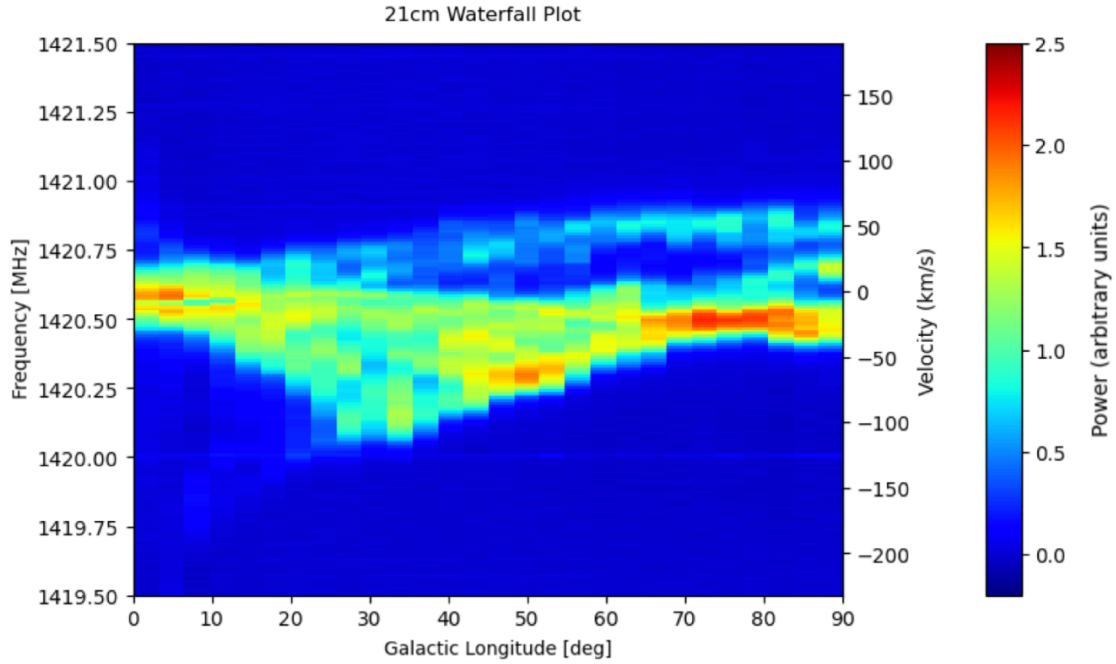


Figure 3: This shows a waterfall plot of 21 cm data as a function of the Galactic longitude (horizontal axis) and observed frequency (left vertical axis). A secondary y-axis on the right shows the corresponding radial velocity in  $\text{km s}^{-1}$ . The colour scale indicates the measured velocity (or intensity) at each frequency-longitude combination and highlights how the 21 cm line profile varies across the sky.

Figure 3 depicts a two-dimensional visualisation of the 21 cm data with Galactic longitude along the horizontal axis and observed frequency on the left vertical axis. The colour scale represents either the measured velocity or intensity while the right vertical axis converts frequency into radial velocity. This allows the tracing of the 21 cm line profile shifts across different longitudes and also reveals structures that could possibly indicate spiral arm crossings or local HI clouds moving toward or away from us. The clear "butterfly" like variation in colour near 1420.4 MHz indicates exactly how the Doppler shift changes with longitude and is consistent with differential Galactic rotation. Overall, the given plot provides an immediate visual image of the Galactic HI distribution and highlights regions of enhanced or diminished emission as a function of both the longitude as well as radial velocity.

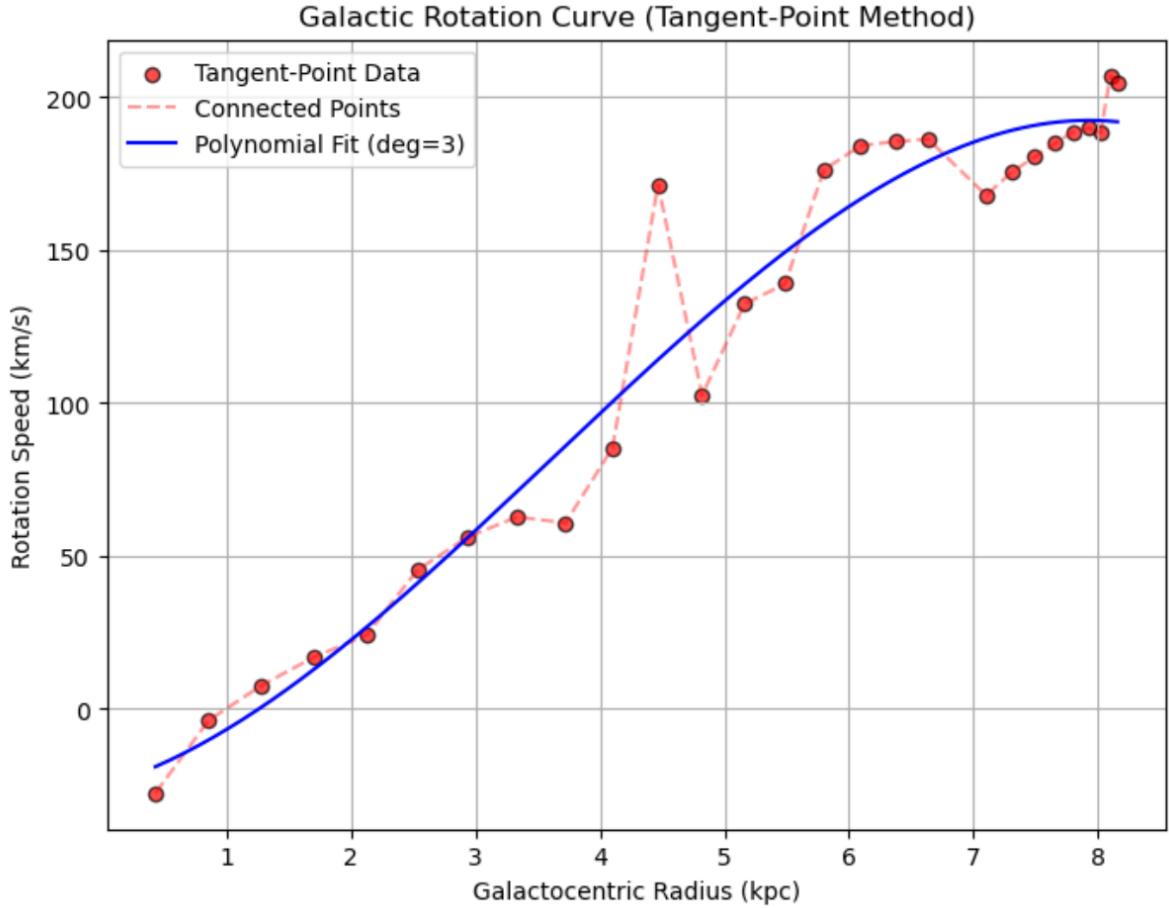


Figure 4: Plot of tangent-point rotation curve of the Milky Way. The red circles depict the observed data points which were derived using the tangent point method and then subsequently connected by a dashed red line. The blue curve is a cubic polynomial fit ( $\text{deg}=3$ ) which provides a smooth approximation to the measured rotation speeds as a function of Galactocentric radius. The overall shape suggests that the rotational velocity increases to around  $200\text{--}240\text{ km s}^{-1}$  near the solar circle (8 kpc), again consistent with the presence of an extended mass distribution beyond the central bulge.

Figure 4 shows the *tangent-point rotation curve* of the Milky Way, with red circles marking the measured rotation speeds as a function of Galactocentric radius. These points are connected by a dashed red line and the smooth blue curve represents a *cubic polynomial fit* (degree = 3) to the data. The horizontal axis spans radii from the central bulge all the way out to around 8 kpc (near the Sun's orbit) and the vertical axis indicates orbital velocity in  $\text{km s}^{-1}$ . The data reveal that the rotational velocity rises from below  $100\text{ km s}^{-1}$  at small radii to around  $200\text{--}240\text{ km s}^{-1}$  near 8 kpc, which is a shape consistent with a mass distribution extending well beyond the visible stellar disk. The polynomial fit tracks the general trend, whereas the deviations between the data and the model can reflect measurement noise or even spiral-arm streaming motions. Overall, the curve's flat or gently rising behaviour at large  $R$  is a very typical indicator of dark matter, implying that the Galaxy's gravitational potential is dominated by a massive, extended halo.

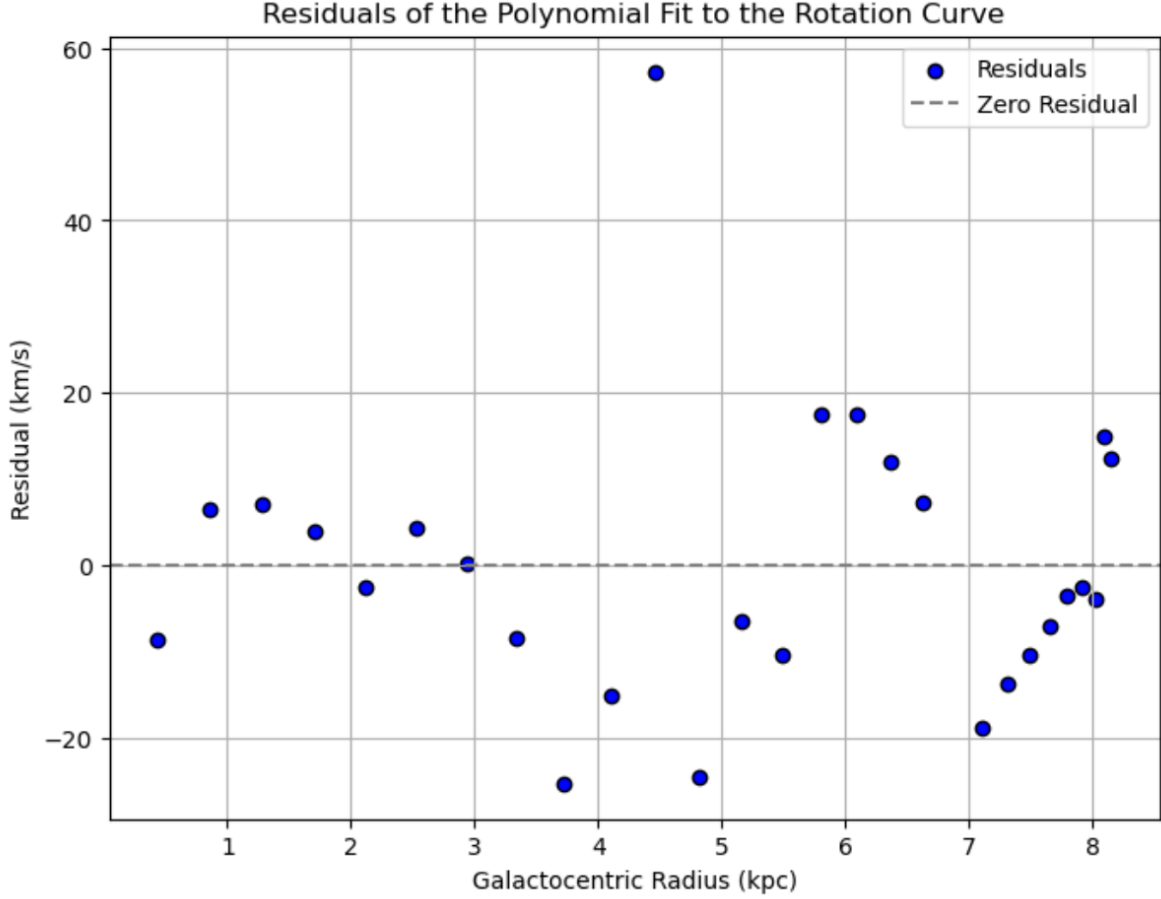


Figure 5: Plot of residuals between the observed rotation speeds and the cubic polynomial fit to the tangent-point data which is then plotted as a function of Galactocentric radius. The horizontal dashed line marks the zero-residual level. Positive residuals indicate data points above the model, while negative residuals lie below. The spread and relatively random pattern of these residuals provides insights into measurement uncertainties, spiral arm streaming motions, and other local deviations from the smooth rotation curve.

Figure 5 presents the residuals between the measured tangent-point rotation speeds and a cubic polynomial fit, plotted against Galactocentric radius. Positive values signify where the observed velocities exceed the model, while negative values indicate the underestimates by the polynomial. Although the overall rotation curve rises and then appears to level off near the 8 kpc mark, the residuals reveal systematic deviations in certain radial ranges. Particularly, the cluster of positive residuals at smaller radii could suggest local dynamical effects such as spiral arm streaming motions, while the more negative values near 7 kpc could reflect either a slight mismatch in the assumed fit or observational uncertainties. A typical Milky Way rotation curve is expected to increase from near zero all the way up to about  $200\text{--}240\text{ km s}^{-1}$  and then remain relatively flat. The polynomial model is able to capture much of this behaviour, but the pattern of residuals highlights that a single cubic function may not perfectly be able to reproduce every feature of the data. Additional factors such as non axisymmetric structures, gas flows, or dark matter substructure could also account for the observed scatter. However, the random distribution of the points around the  $y=0$  line with the exception of the outlier at approximately 4.5 kpc indicates a decent fit.

In a purely centrally concentrated mass distribution such as one dominated by a dense bulge at small radii, orbital velocities typically follow a Keplerian decline, decreasing as  $R^{-1/2}$  once beyond the central mass. In contrast, our measured rotation curve remains relatively flat or gently rising up to at least 8 kpc. This behaviour potentially signals that the Galaxy’s gravitational potential extends well beyond the luminous bulge and disk and requires additional, unseen mass to maintain these high orbital speeds. Consequently, it can be inferred that the Milky Way possesses a massive, extended halo which can be most naturally explained by the presence of dark matter which dominates the gravitational potential

at large radii. Therefore, instead of being confined to the central regions, a substantial fraction of the Galaxy's mass is distributed throughout this halo and drives the near constant or slowly rising rotation curve beyond the central bulge.

Although the bulk of the Milky Way's luminosity arises from its central bulge, the rotation curve in Figure 4 does not mirror a mass distribution confined to that region. In a scenario where mass strictly follows light it would be expected that the rotation speed would peak near the centre and then decline in a Keplerian manner at larger radii. Instead, our observed rotation curve remains flat or only gently declines beyond the initial central bulge. This inconsistency then implies that the Galaxy's gravitational potential is not solely dictated by the luminous matter. An alternate explanation is that a substantial amount of mass is distributed in a dark matter halo that envelops the entire Galaxy. Even though this halo is not directly visible, it contributes the extra gravitational pull needed to sustain high orbital velocities in the outer regions, thereby reconciling the flat rotation curve with the observed distribution of light.

## 5 Discussion & Conclusion

In this lab, 21 cm spectral observations were used and the tangent point method to derive the Milky Way's rotation curve. The data reduction process included baseline subtraction, conversion of frequency to radial velocity and peak detection to isolate the maximum velocity component at each Galactic longitude. The resulting rotation curve plotting the rotation speed against Galactocentric radius, does not exhibit a Keplerian decline as would be expected if the mass were predominantly concentrated in the central bulge. Instead, the rotation speed remains nearly flat (at approximately 200–240 kms near the solar circle which implies a gravitational potential that extends well beyond the luminous regions of the Galaxy).

The cubic polynomial fit to our data was chosen for its balance between flexibility and simplicity. It successfully captured the steep rise in rotational velocity at small radii and the subsequent flattening at larger radii. Nonetheless, the residuals of the fit also revealed systematic deviations that could be attributed to local dynamical effects, such as spiral arm streaming motions or uncertainties in the baseline subtraction and peak selection processes. These discrepancies highlight the importance of further refinement in error quantification and also data calibration.

These findings suggest that despite the bulk of the Milky Way's luminosity emanating from the central bulge, the rotation curve remains inconsistent with a mass distribution that strictly follows the light. Instead, the persistent high rotational speeds at large radii indicate the presence of an extended dark matter halo which plays a crucial role in the Galaxy's overall gravitational potential. This conclusion is in line with established theoretical models and previous observations of spiral galaxies.

Looking forward, additional pointings, improved baseline removal techniques, and more advances fitting methods such as multi component models could potentially help enhance the precision of the rotation curve. Such refinements would allow for a more detailed exploration of the Galactic mass distribution and provide tighter constraints on the properties of the dark matter halo.

In summary, our results confirm that the Milky Way's rotation curve is dominated by an extended mass component which is most naturally interpreted as dark matter rather than being solely determined by the centrally concentrated stellar bulge. This experiment reinforces the need for dark matter in explaining Galactic dynamics along with highlighting avenues for future improvement in observational and data reduction methodologies.

## 6 Bibliography

Department of Astronomy and Astrophysics, *Mapping the Milky Way*: Lab Manual for AST325/326 (Winter 2025), University of Toronto, March 2025.



## Appendix:

### A Derivations

#### A.1. Conversion from Frequency to Radial Velocity

The Doppler shift for non-relativistic velocities allows conversion from observed frequency  $f$  into a radial velocity  $v$ . Starting with the relation

$$\frac{\Delta f}{f_0} = \frac{f_0 - f}{f_0} \approx \frac{v}{c},$$

where  $f_0 = 1420.4$  MHz is the rest frequency of the 21 cm line and  $c$  is the speed of light. This equation is rearranged to obtain

$$v = c \frac{f_0 - f}{f_0}.$$

This equation forms the basis for converting the measured spectrum from frequency space into radial velocity space.

#### A.2. Tangent-Point Method for the Galactic Rotation Curve

In the first Galactic quadrant ( $0^\circ < l < 90^\circ$ ) the tangent point is defined as the location along the line-of-sight where the distance to the Galactic centre is minimised. At the tangent point, the Galactocentric radius  $R$  is given by

$$R = R_0 \sin(l),$$

where  $R_0$  is the Sun's distance from the Galactic centre and  $l$  is the Galactic longitude. The maximum observed radial velocity  $v_{\text{los}}$  at this point is used to compute the circular rotation speed using the relation

$$V(R) = v_{\text{los}} + V_0 \sin(l),$$

with  $V_0$  being the local circular speed at the Sun's orbit. This derivation comes from the geometry of circular motion in the Galactic plane where the line of sight velocity is maximised at the given tangent point.

## B Code

### B.0.1 Code for Converting Galactic Coordinates to Equatorial and Horizon Coordinates

```
1 # importing the libraries
2 import numpy as np
3 import pandas as pd
4 from astropy.coordinates import SkyCoord, EarthLocation, AltAz
5 from astropy.time import Time
6 import astropy.units as u
7
8 # defining the current location
9 obs_loc = EarthLocation(lat=43.7*u.deg, lon=-79.4*u.deg, height=76*u.m)
10
11 # create variable for observation time (9:30 AM EST = 14:30 UTC on February 24, 2025)
12 obs_start = Time('2025-02-24 14:30:00')
13
14 # defining observation interval (around 1.5 minutes each)
15 obs_interval = 1.5 * u.min
16
17 # define the Galactic coordinates (l, b)
18 l_values = np.arange(3, 84, 3) # every 3 degrees
19 b_values = np.zeros_like(l_values) # all at b = 0
20
21 # now initialise lists for storing results
22 ra_list, dec_list, alt_list, az_list, time_list = [], [], [], [], []
23
24 # converting Galactic to Equatorial and then to Horizon coordinates
25 for i, (l, b) in enumerate(zip(l_values, b_values)):
26     # Galactic to Equatorial
27     galactic_coord = SkyCoord(l=l*u.deg, b=b*u.deg, frame='galactic')
```

```

28 equatorial_coord = galactic_coord.transform_to('icrs') # to RA, Dec
29
30 # the time for each pointing
31 obs_time = obs_start + i * obs_interval
32 # conversion to Horizon coordinates
33 altaz_frame = AltAz(obstime=obs_time, location=obs_loc)
34 horizon_coord = equatorial_coord.transform_to(altaz_frame)
35
36 # store results in empty lists
37 ra_list.append(equatorial_coord.ra.deg)
38 dec_list.append(equatorial_coord.dec.deg)
39 alt_list.append(horizon_coord.alt.deg)
40 az_list.append(horizon_coord.az.deg)
41 time_list.append(obs_time.iso)
42
43 # creating dataframe
44 df_updated = pd.DataFrame({
45     'Time (UTC)': time_list,
46     'Galactic l (deg)': l_values,
47     'Galactic b (deg)': b_values,
48     'RA (deg)': ra_list,
49     'Dec (deg)': dec_list,
50     'Alt (deg)': alt_list,
51     'Az (deg)': az_list
52 })
53 # Display the updated data
54 print(df_updated)

```

Listing 1: Python code for converting Galactic coordinates to Equatorial and Horizon coordinates

## B.0.2 Code to Plot 21 cm Spectra

```

1 import numpy as np
2 import struct
3 import matplotlib.pyplot as plt
4
5 # format of the file name
6 start_str = "output"
7 mid_str_1 = "000"
8 mid_str_2 = "00"
9 end_str = ".dat"
10 filenames = []
11
12 # constants
13 c = 299792.458 # light speed in km/s
14 f0 = 1420.4 # rest frequency of HI line in MHz
15
16 for i in range(28):
17     if i < 10:
18         filename = start_str + mid_str_1 + str(i) + end_str
19     else:
20         filename = start_str + mid_str_2 + str(i) + end_str
21     filenames.append(filename)
22
23 # plot spectra on the same plot
24 plt.figure(figsize=(10, 6))
25 for file in filenames:
26     with open(file, 'rb') as f:
27         nf, nt, alt, az = struct.unpack('iiff', f.read(16))
28         lf = np.fromfile(f, dtype=np.float32, count=nf) # Frequency list
29         lt = np.fromfile(f, dtype=np.float64, count=nt) # Time list
30         sp = np.fromfile(f, dtype=np.float32, count=nf) # Spectrum
31         bl = np.fromfile(f, dtype=np.float32, count=nf) # Baseline
32         wf = np.fromfile(f, dtype=np.float32, count=nf * nt) # Waterfall data
33         # removing polynomial fit baseline
34         spectrum_corrected = sp - bl
35         # convert frequency to radial velocity
36         velocity = c * (f0 - lf) / f0 # the Doppler shift equation
37         # plotting spectrum
38         plt.plot(velocity, spectrum_corrected, label=f'Alt: {alt:.1f}, Az: {az:.1f}')
39
40 # plotting settings

```

```

41 plt.xlabel("Radial Velocity (km/s)")
42 plt.ylabel("Power (arbitrary units)")
43 plt.ylim(-2, 2.5)
44 plt.title("21cm Spectra from Different Pointings")
45 plt.grid()
46 plt.gca().invert_xaxis() # inverting x-axis so approaching gas comes from left
47 plt.show()

```

Listing 2: Python code for plotting the 21 cm spectra from different pointings

### B.0.3 Code to Compute and Plot the Galactic Rotation Curve and Residual Graph

```

1 # import required libraries
2 import numpy as np
3 import struct
4 import matplotlib.pyplot as plt
5 from scipy.signal import find_peaks
6 import pandas as pd
7
8 # Constants
9 c = 299792.458 # Speed of light in km/s
10 f0 = 1420.4 # Rest frequency of HI line in MHz
11 R0 = 8.2 # kpc, distance of Sun from Galactic center
12 V0 = 220.0 # km/s, local circular speed at R0
13 VEL_MIN = -300.0
14 VEL_MAX = 300.0
15
16 # Naming scheme & Galactic longitudes
17 start_str = "output"
18 mid_str_1 = "000"
19 mid_str_2 = "00"
20 end_str = ".dat"
21 n_files = 28
22 galactic_longitudes = np.linspace(3, 84, n_files)
23 filenames = []
24 for i in range(n_files):
25     if i < 10:
26         filename = f"{start_str}{mid_str_1}{i}{end_str}"
27     else:
28         filename = f"{start_str}{mid_str_2}{i}{end_str}"
29     filenames.append(filename)
30
31 # Data storage for tangent-point results
32 tp_data = []
33
34 # Process each file and apply the Tangent-Point Method
35 for i, file in enumerate(filenames):
36     with open(file, 'rb') as f:
37         nf, nt, alt, az = struct.unpack('iiff', f.read(16))
38         lf = np.fromfile(f, dtype=np.float32, count=nf)
39         lt = np.fromfile(f, dtype=np.float64, count=nt)
40         sp = np.fromfile(f, dtype=np.float32, count=nf)
41         bl = np.fromfile(f, dtype=np.float32, count=nf)
42         wf = np.fromfile(f, dtype=np.float32, count=nf * nt)
43         # Subtract the polynomial fit baseline
44         spec2 = sp - bl
45         # Convert frequency to radial velocity (km/s) using the Doppler shift equation
46         velocity = c * (f0 - lf) / f0
47         # Restrict to 300 km/s
48         mask = (velocity >= VEL_MIN) & (velocity <= VEL_MAX)
49         velocity_masked = velocity[mask]
50         spec_masked = spec2[mask]
51         # Find peaks in the masked region
52         peaks, peak_props = find_peaks(
53             spec_masked,
54             height=1.0,
55             prominence=0.5,
56             distance=5
57         )
58         # For the tangent-point method (first quadrant): choose the maximum velocity peak
59         l_deg = galactic_longitudes[i]
60         l_rad = np.radians(l_deg)

```

```

61     if 0 < l_deg < 90 and len(peaks) > 0:
62         max_peak_idx = peaks[np.argmax(velocity_masked[peaks])]
63         v_los_tangent = velocity_masked[max_peak_idx]
64         R_tangent = R0 * np.sin(l_rad)
65         V_tangent = v_los_tangent + V0 * np.sin(l_rad)
66         tp_data.append({
67             "Galactic Longitude (deg)": l_deg,
68             "Altitude": alt,
69             "Azimuth": az,
70             "Radial Velocity (km/s)": v_los_tang

```

Listing 3: Python code for computing and plotting the Galactic Rotation Curve using the tangent-point method and its residual graph